Animal Nutrition 20 (2025) 226–238

Contents lists available at ScienceDirect

Animal Nutrition

journal homepage: http://www.keaipublishing.com/en/journals/aninu/

Original Research Article

Transcriptome analysis reveals modulations in glycosylation profiles of the mucosal barrier and their potential interaction with gut microbiota in weaned piglets

Hao Cheng [a, b], Hao Li [a, b, †], Yujie Zhao [a, b], Kai Yang [a, b], Jing Wang [a, b], Bie Tan [a, b, *], Xiaokang Ma [a, b, *]

[a] College of Animal Science and Technology, Hunan Agricultural University, Changsha 410128, China
[b] Yuelushan Laboratory, Changsha 410128, China

ARTICLE INFO

Article history:
Received 7 April 2024
Received in revised form
9 July 2024
Accepted 2 December 2024
Available online 10 December 2024

Keywords:
Glycosylation profiles
Bacterial community
Mucosal immunity
Post-weaned piglet

ABSTRACT

The current study aims to investigate the potential interaction between glycosylation profiles of the Ningxiang breed (NX) and Western Duroc × Landrace × Yorkshire breed (DLY) weaned piglets, and their characteristic microbes, employing integrated analyses of transcriptomics and metagenomics. Twenty-four (12 NX and 12 DLY) at 28 days of age were transported into an experimental house and fed the same weaned piglet diet. The trail period was 7 days. Results revealed that the NX piglets had a higher growth-to-feed ratio, body weight gain scale, and lower pathological score of intestinal injury compared with the DLY piglets ($P < 0.01$). DLY piglets displayed elevated mRNA expression levels of *MUC2* and *MUC5AC* in colonic mucosal tissue than NX piglets ($P < 0.05$). Within the O-linked glycosylated differentially expressed genes (DEGs), *FNTA*, *GALNT18*, *POMGNT1*, *POMGNT2*, and *POMT1* were significantly upregulated in DLY piglets relative to NX piglets ($P < 0.05$). Conversely, *C1GALT2*, *GALNT1*, *KMT2C*, and *OGT* were significantly downregulated in DLY piglets compared to NX piglets ($P < 0.05$). The *KMT2C* gene was hardly expressed in the transcriptome of DLY piglets. At the phylum taxonomic level, NX piglets had a higher abundance of Firmicutes, while DLY piglets had a higher abundance of Proteobacteria. At the genus taxonomic level, NX piglets had a higher abundance of *Lactobacillus*, whereas DLY piglets had a higher abundance of *Collinsella*, *Enterococcus* and *Escherichia*. The results of the correlation between intestinal differential bacteria and O-chain glycosylated DEG showed that *C1GALT2*, *GALNT1* and *KMT2* were associated with *Lactobacillus_pontis* showed a positive correlation ($R = 0.67$). Through comparative analysis of differentially glycosylated genes and their associated functions, this study highlights the potential role of reduced expression of *GALNT1* and *KMT2C* genes, involved in O-linked protein and glycan reactions, in impairing the intestinal barrier function of DLY piglets. Furthermore, members of the *Lactobacillus* and *Prevotella* genera may actively contribute to the regulation of piglet colon glycosylation profiles.

1. Introduction

The post-weaning syndrome among piglets represents a significant challenge in the modern pig industry, impacting profitability. Multiple factors contribute to symptoms such as diarrhea and growth retardation in post-weaning piglets, including changes in diet, environment and other factors, among which the gut microbiota plays a key role (Han et al., 2024). Piglets with weaning syndrome had reduced beneficial bacterium, such as *Lactobacillus* and *Faecalibacterium*, and increased opportunistic pathogens, mainly Proteobacteria, namely *Escherichia_coli* (*E.coli*) (Frese et al., 2015;

* Corresponding authors.
E-mail addresses: bietan@hunau.edu.cn (B. Tan), maxiaokang@hunau.edu.cn (X. Ma).
† The author has contributed equally to this work.
Peer review under the responsibility of Chinese Association of Animal Science and Veterinary Medicine.

Production and Hosting by Elsevier on behalf of KeAi

https://doi.org/10.1016/j.aninu.2024.12.001

Gresse et al., 2019). The dysbiosis of the gut microbiome, coupled with elevated pro-inflammatory substances, exacerbates the inflammatory response in piglet guts, hindering the alleviation of weaning stress symptoms (Kostic et al., 2014; Morgan et al., 2012).

Significant questions arise concerning how interactions between host genes and microbiome occur, and what are these intricate interactions between host genes and the microbiome within the gut of weaned piglets. Epithelial glycans, which form a crucial component of the intestinal mucosa, play a pivotal role in this complex communication. These glycans not only provide essential ligands and nutrients, but also act as a vital interface, mediating the dynamic dialogue between gut microbes and the host organism. This intricate relationship is fundamental to understanding the mechanisms that underpin gut health and development in weaned piglets (Arora et al., 2024; Kudelka et al., 2020). Therefore, the epithelial glycans are essential cues for orchestrating host–microbial interactions (Goto et al., 2014; Demirturk et al., 2024). Although free-form glycans are also present, they are more commonly secreted by the intestinal mucosa in the form of glycoproteins, primarily mucins (Cummings, 2019).

The process of glycan synthesis and attachment to peptide chains, resulting in glycoproteins, is known as glycosylation, and it profoundly affects the conformation and function of glycoproteins (Neelameghans, 2016). There are 2 major classes of glycan-protein linkages, namely N-linked glycans (N-glycans) and O-linked glycans (O-glycans) (Cummings and Pierce, 2014). Specific glycosylation processes enable mucin to exert immune responses against specific pathogens. Mucin sulfation and sialylation, orchestrated by interleukin (IL)-13/IL-4R, contribute to the expulsion of worms and nematodes from the intestine (Earley et al., 2019). Research has indicated a substantial reduction in mucin sulfation in patients with ulcerative colitis (Kawashima, 2012). Consequently, specific alterations in glycosylation profile have become the diagnostic basis of intestinal inflammation (Grous et al., 2020; Nagao et al., 2020). Moreover, accumulating evidence revealed the regulation of glycosylation contributes to the remedy of human inflammatory bowel diseases (IBDs) (Kudelka et al., 2020).

Ningxiang pigs are renowned native Chinese pigs that retain resistance to post-weaning stress throughout their long domestication history, partly due to their unique gut microbiota (Ma et al., 2022). Recognizing the pivotal role of glycosylation profiles in gut immunity and their close association with gut microbes, this study aims to investigate the potential interaction between glycosylation profiles in Ningxiang breed (NX) and Western Duroc × Landrace × Yorkshire breed (DLY) weaned piglets, along with their characteristic microbial communities. This investigation will be based on integrated analyses of transcriptomics and metagenomics.

2. Materials and methods

2.1. Animal ethics statement

All animal handling and all procedures of this study have received approval from the Animal Care and Use Ethics Committee of the Hunan Agricultural University (approval number CACAHU, 2021-01106, Changsha, China). The experiment complied with the Animal Research: Reporting of in vivo Experiments (ARRIVE) guidelines.

2.2. Animal experiment design

Synchronously, twenty-four 28-day-old barrows (12 NX and 12 DLY) were transported into an experimental house and fed the same weaned piglet diet formulated according to the NRC (2012) recommendations as shown in Table 1. Briefly, values of digestible energy (DE), and available phosphorus were calculated using data provided by the Feed Database in China (2019). Each piglet was housed in a separate cage to ensure that the gut microbiota did not interfere with each other. A 7-day rearing period followed, allowing the piglets to acclimate to their new environment and minimize stress induced during transport.

Table 1
Ingredients and nutrient levels of the diets (%, as-fed basis)

Item	Content
Ingredients	
Corn	23.93
Extruded corn	35.00
Soybean	8.00
Fermented soybean	9.00
Whey powder	6.00
Fish meal	4.00
Whey powder	2.00
Soybean oil	1.00
Glucose	3.00
Sucrose	2.00
L-Lysine	0.40
DL-Methionine	0.11
L-Threonine	0.12
L-Alanine	1.59
Carrier	0.90
Organic acid calcium	0.60
$CaHPO_4$	1.00
Choline chloride (50%)	0.01
Antioxidant	0.05
Mineral premix[1]	0.15
Vitamin premix[2]	0.04
ZnO	0.40
Acidifier	0.70
Total	100.00
Calculated composition	
Digestible energy, kcal/kg	3445.60
Available phosphorus	0.40
Analyzed composition	
Crude protein	18.37
Ether extract	5.23
Soluble dietary fiber	1.30
Insoluble dietary fiber	12.80
Calcium	0.47
Total phosphorus	0.54

[1] Mineral premix provided for 1 kg diet: Zn (ZnO), 50 mg; Cu ($CuSO_4$), 20 mg; Mn (MnO), 55 mg; Fe ($FeSO_4$), 100 mg; I (KI), 1 mg; Co ($CoSO_4$), 2 mg; Se (Na_2SeO_3), 0.3 mg.

[2] Vitamin premix provided for 1 kg diet: vitamin A, 8255 IU; vitamin D_3, 2000 IU; vitamin E, 40 IU; vitamin B_1, 2 mg; vitamin B_2, 4 mg; pantothenic acid, 15 mg; vitamin B_6, 10 mg; vitamin B_{12}, 0.05 mg; nicotinic acid, 30 mg; folic acid, 2 mg; vitamin K_3, 1.5 mg; biotin, 0.2 mg; choline chloride, 800 mg; and vitamin C, 100 mg.

Throughout the experiment, the initial and final weights of each piglet were recorded, along with their daily feed consumption. Additionally, the daily diarrhea rate for each breed of piglets was determined by assessing the fecal consistency score (Li et al., 2021). All piglets were housed in an environmentally controlled nursery facility with slatted plastic flooring and a mechanical ventilation system, and had free access to drinking water (ambient temperature from 21 to 27 °C).

2.3. Sample collection

Eight piglets in each group closest to the average group bodyweight (8.1 ± 0.4 kg) were humanely killed by intramuscular injection of xylazine hydrochloride (Jilin Huamu Animal Health Product Co., Ltd., Changchun, China) at a dosage of 0.5 mL/kg body weight on day 7. The dissection process involved a longitudinal incision along the abdomen, followed by the isolation of middle colon segments to collect mucosal and digesta samples. These samples were promptly snap-frozen in liquid nitrogen and then

shipped to −80 °C on dry ice. The mucosal samples were used for transcriptome sequencing analysis, whereas digesta samples were used for metagenomic sequencing analysis. Moreover, adjacent colonic tissue was excised and gently rinsed to remove the contents and stored at room temperature in Carnoy's fixative for paraffin sectioning and Periodic Acid-Schiff (PAS) stain.

2.4. Microscopic morphology

The preparation of paraffin sections and the PAS staining protocol were as reported by Xia et al. (2022). In addition, the staining ratio of Schiff's reagent was assessed using image-J, and pathological scoring was performed according to the method of Zhai et al. (2018).

2.5. RNA extraction and sequencing

Total RNA was extracted from the tissue using TRIzol Reagent according to the manufacturer's instructions (Invitrogen), and genomic DNA was removed using DNase I (TaKaRa). Then RNA quality was determined by 2100 Bioanalyser (Agilent) and quantified using the ND-2000 (NanoDrop Technologies). Only high-quality RNA sample (OD260/280 = 1.8–2.2, OD260/230 ≥ 2.0, RNA integrity number (RIN) ≥ 6.5, 28S:18S ≥ 1.0, >1 μg; $n = 6$ per group) was used to construct sequencing library. RNA-seq transcriptome library was prepared following TruSeq RNA sample preparation Kit from Illumina (San Diego, CA) using 1 μg of total RNA. Shortly, mRNA was isolated according to polyA selection method by oligo(dT) beads and then fragmented by fragmentation buffer. Double-stranded cDNA was synthesized using a SuperScript double-stranded cDNA synthesis kit (Invitrogen, CA) with random hexamer primers (Illumina). Then the synthesized cDNA was subjected to end-repair, phosphorylation and 'A' base addition according to Illumina's library construction protocol. Libraries were selected for cDNA target fragments of 300 bp on 2% Low Range Ultra Agarose followed by PCR amplified using Phusion DNA polymerase (NEB) for 15 PCR cycles. After quantification by TBS380, the paired-end RNA-seq sequencing library was sequenced with the Illumina HiSeq xten/NovaSeq 6000 sequencer (2 × 150 bp read length).

2.6. Differential expression analysis and functional enrichment for transcriptome

To identify differentially expressed genes (DEGs) between 2 different samples, the expression level of each transcript was calculated according to the transcripts per million reads (TPM) method. RSEM (http://deweylab.biostat.wisc.edu/rsem/) was used to quantify gene abundances. Briefly, differential expression analysis was performed using the DESeq2/DEGseq/EdgeR with Q value ≤ 0.05, DEGs with |log2FC| > 1 and Q value ≤ 0.05 (DESeq2 or EdgeR)/Q value ≤ 0.001 (DEGseq) were considered to be significantly DEGs). In addition, functional-enrichment analysis including Gene Ontology (GO) and Kyoto Encyclopedia of Genes and Genomes (KEGG) were performed to identify which DEGs were significantly enriched in GO terms and metabolic pathways at BH-corrected *P*-value ≤0.05, compared with the whole-transcriptome background. GO functional enrichment and KEGG pathway analysis were carried out by Goatools (https://github.com/tanghaibao/Goatools) and KOBAS (http://kobas.cbi.pku.edu.cn/home.do).

2.7. DNA extraction, library construction, and metagenomic sequencing

According to manufacturer's instructions, the total genomic DNA was extracted from colon samples using the E.Z.N.A. Soil DNA Kit (Omega Bio-tek, Norcross, GA, USA). The extracted DNA concentration and purity was determined with TBS-380 and NanoDrop2000, respectively. DNA extract quality was checked on 1% agarose gel. DNA extract was fragmented to an average size of about 400 bp using Covaris M220 (Gene Company Limited, China) for paired-end library construction. Paired-end library was constructed using NEXTFLEX Rapid DNA-Seq (Bioo Scientific, Austin, TX, USA). Adapters containing the full complement of sequencing primer hybridization sites were ligated to the blunt end of fragments. Paired-end sequencing was performed on Illumina NovaSeq/Hiseq Xten (Illumina Inc., San Diego, CA, USA) at Majorbio BioPharm Technology Co., Ltd. (Shanghai, China) using NovaSeq Reagent Kits/HiSeq X Reagent Kits according to the manufacturer's instructions (www.illumina.com).

Open reading frames (ORFs) from each assembled contig were predicted using MetaGene (http://metagene.cb.k.u-tokyo.ac.jp/). The predicted ORFs with a length being or over 100 bp were retrieved and translated into amino acid sequences using the NCBI translation table (http://www.ncbi.nlm.nih.gov/Taxonomy/taxonomyhome.html/index.cgi?chapter=tgencodes#SG1). A non-redundant gene catalog was constructed using CD-HIT (http://www.bioinformatics.org/cd-hit/, version 4.6.1) with 90% sequence identity and 90% coverage. Reads after quality control were mapped to the non-redundant gene catalog with 95% identity using SOAPaligner (http://soap.genomics.org.cn/, version 2.21), and gene abundance in each sample were evaluated. Representative sequences of non-redundant gene catalog were aligned to the NCBI NR database with an e-value cutoff of 1e-5 using Diamond (http://www.diamondsearch.org/index.php, version 0.8.35) for taxonomic annotations.

2.8. Association analysis for bioinformatics

A random forest-based machine learning approach regression model was established between differentially glycosylated genes and signaling gene expression in the categories of the immune system or signal transduction based on the KEGG database. Briefly, the highly correlated features were further filtered with the findCorrelation function from R package "caret". The randomForest function from R package "randomForest" was carried out to train the model with 500 estimator trees and "mtry" was left as the default setting. Predictions and performance metrics were calculated using the "predict" and "prediction" performance functions from R package "ROCR". Each glycosylation gene obtained 5 models by assembling the training datasets with sampling ratios of 65%, 70%, 75%, 80%, and 85%, respectively. Then, the models with the highest R-square were selected for the final prediction and extracted associated signal genes. Total associated signal genes for each glycosylation gene were subjected to enrichment analysis of the KEGG signaling pathway (Benjamini-Hochberg (BH) adjusted *P*-value <0.05 to judge rich factor was statistically significant).

2.9. Statistical analysis

Body weight and gene expression data were analyzed by the unpaired *t*-test procedure of SPSS 21.0 (SPSS Inc., Chicago, IL, USA), and each piglet was regarded as a statistical unit. Data are shown as mean values with standard error (SEM). The chi-square test was used to analyze the diarrhea rate in piglets. Statistical significance was declared when $P < 0.05$. Correlations were analyzed by using Spearman's correlation in R.4.0.5 (The R Foundation) with the RStudio package. Correlation results were corrected by False Discovery Rte (FDR) analysis according to the Benjamini-Hochberg procedure, with $\alpha < 0.05$.

3. Results

3.1. Growth performance

The growth performance and diarrhea rate of piglets have been shown in Fig. 1 and Table 2. Compared with the DLY piglets, the NX piglets had higher feed conversation ratio and body weight gain scale ($P < 0.001$).

3.2. Microscopic morphology and secretory mucin gene expression of colonic tissue

PAS-stained sections of piglet colon tissue are shown in Fig. 2A. Compared with DLY piglets, NX piglets had a larger stained area of Schiff's reagent and a lower pathological score of intestinal injury ($P < 0.05$). The expression levels of secreted mucin genes in colonic mucosa are illustrated in Fig. 2B. DLY piglets exhibited higher expression levels of *MUC2* and *MUC5AC* than NX piglets ($P < 0.05$), while no significant difference was observed in *MUC5B* expression between the 2 groups ($P < 0.05$).

3.3. Transcriptional profile of colonic tissue

A total of 501.81 million (with an average of 41.82 ± 1.36 million reads per sample) high-quality paired reads were generated from the 12 colon tissue samples, with an overall read alignment rate to the *Ovis aries* reference genome of (81 ± 2.22)%. Among these, 5771 genes that were significantly differentially expressed in the DLY piglets compared with the NX piglets, including 2223 upregulated and 3548 downregulated genes ($P < 0.05$) (Fig. 3A). According to the functional annotation of GO and KEGG databases, a total of 218 mRNAs from 92 glycosylation genes were identified in piglets. By intersecting the mRNA of the glycosylated genes with the differential transcriptome, 83 glycosylation DEGs were identified using the Venn map (Fig. 3B).

3.4. Function analysis in glycosylation DEGs

Glycosylated DEGs of DLY and NX piglets are presented in Fig. 4A. Glycosylated DEGs upregulated in NX piglets were found to be enriched in biological processes, including protein O-linked glycosylation, among others, in comparison to DLY piglets (Fig. 4B). Conversely, glycosylated DEGs downregulated in NX piglets enriched in biological processes including N-glycan processing etc., compared to DLY piglets (Fig. 4C). Moreover, among all O-linked glycosylated DEGs, *FNTA*, *GALNT18*, *POMGNT1*, *POMGNT2* and *POMT1* were significantly upregulated in DLY piglets compared with NX piglets, whereas *C1GALT2*, *GALNT1*, *KMT2C* and *OGT* were significantly downregulated in DLY piglets compared with NX piglets ($P < 0.05$) (Fig. 4D).

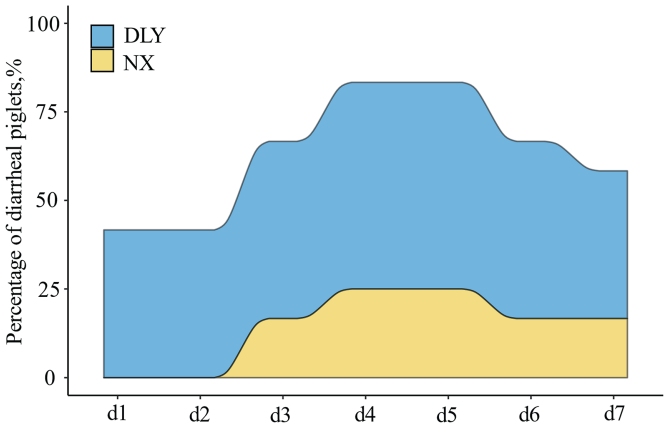

Fig. 1. Diarrheal rate in NX and DLY piglets. DLY = Duroc × Landrace × Yorkshire breed; NX = Ningxiang breed.

Table 2
Growth performance of NX and DLY piglets.

Item	DLY	NX	*P*-value
Initial weight, kg	7.41 ± 0.092	7.52 ± 0.083	0.099
Final weight, kg	8.09 ± 0.148	9.35 ± 0.191	<0.001
Average daily weight gain, g	96.31 ± 15.449	261.43 ± 20.174	<0.001
Average daily feed intake, g	219.68 ± 26.136	457.50 ± 21.962	<0.001
Feed conversation ratio	2.49 ± 0.168	1.80 ± 0.069	<0.001

DLY = Duroc × Landrace × Yorkshire breed; NX = Ningxiang breed.

3.5. Prediction of upstream signaling pathways of glycosylation DEGs based on random forest regression model

Utilizing the refined random forest regression model, we identified the predictors of glycosylation genes in the transcriptome data and constructed a network to visualize the connections (Fig. S1). X. Particularly, *GALNT1* and *KMT2C*, referred to as *GALNT* in the KEGG database, were found to be closely linked to pathways in the immune system and signal transduction. Pathways in the immune system category that were closely related to *GALNT1* or *KMT2C* included Cytosolic DNA-sensing signaling pathways, retinoic acid-inducible gene 1 (RIG-1) like receptor signaling pathways, Toll-like receptor signaling pathways, C-type lectin receptor signaling pathways, IL-17 signaling pathways, Leukocyte transendothelial migration, Chemokine signaling pathways, Natural killer cell mediated cytotoxicity and NOD-like receptors signaling pathways (Fig. 5A). Pathways in the Signal transduction category closely related to *GALNT1* or *KMT2C* included Notch signaling pathways, Hedgehog signaling pathways, Apelin signaling pathways, ErbB signaling pathways, Hippo signaling pathways, hypoxia-inducible factor (HIF-1) signaling pathways, Janus kinase-siganal transducer and activator of transcription (JAK-STAT) signaling pathways, Mitogen-activated protein kinase (MAPK) signaling pathways, forkhead box O (FoxO) signaling pathways, transforming growth factor β (TGF-beta) signaling pathways, mammalian target of rapamycin (mTOR) signaling pathways, phosphatidylinositol-3-kinase-Akt (PI3K-Akt) signaling pathways, Ras signaling pathways and Tumor necrosis factor (TNF) signaling pathways (Fig. 5B).

Additionally, *C1GALT2* expression was potentially associated with the Toll-like receptor signaling pathway. The expression of *OGT* was potentially associated with Toll and Imd signaling pathway, RIG-1-like receptor signaling pathway and Toll-like receptor signaling pathway. The expression of *MAN2A1* was potentially associated with the cytosolic DNA-sensing pathway, cytokine signaling pathway, Toll and Imd signaling pathway, RIG-1-like receptor signaling pathway, and Toll-like receptor signaling pathway (Fig. 5A).

3.6. Differences in the colonic microbiota between 2 breed piglets

The significant variations in microbiota composition were identified through beta diversity using principal coordinate analysis (PcoA) between the 2 breeds (Fig. 6A). At the phylum taxonomic level, NX piglets exhibited a higher abundance of Firmicutes, while DLY piglets had a greater abundance of Proteobacteria (Fig. 6B). At the genus taxonomic level, NX piglets had a higher abundance of *Lactobacillus*, whereas DLY piglets had a higher abundance of *Collinsella*, *Enterococcus* and *Escherichia* (Fig. 6C).

Further analysis using linear discriminant analysis effect size (LEfSe) revealed species-level taxonomic differences between NX

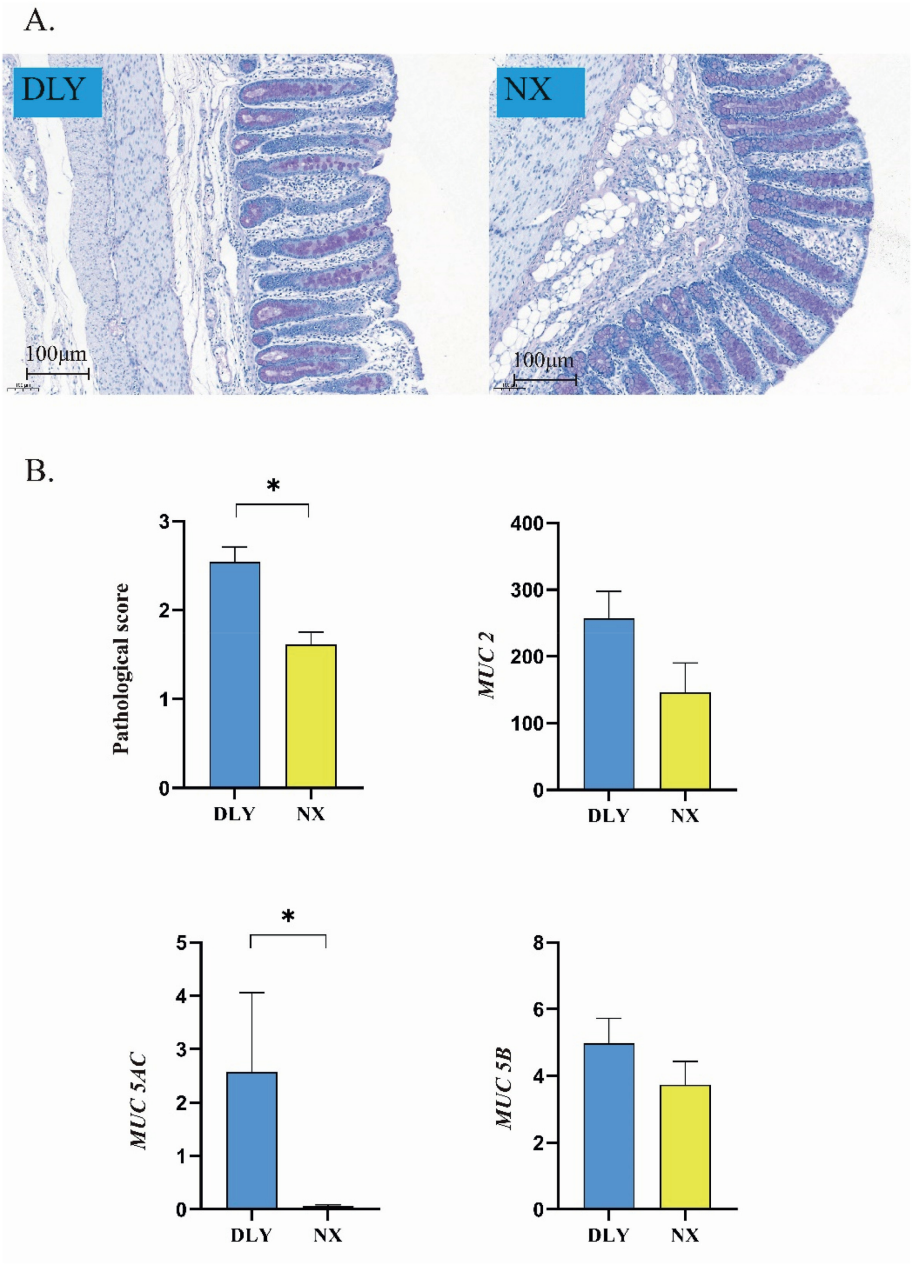

Fig. 2. Microscopic morphology of piglet colon. (A) PAS staining; (B) mRNA expression of secreted mucin. DLY = Duroc × Landrace × Yorkshire breed; NX = Ningxiang breed; PAS = Periodic acid-Schiff stain. ** indicates $P < 0.01$, * indicates $P < 0.05$.

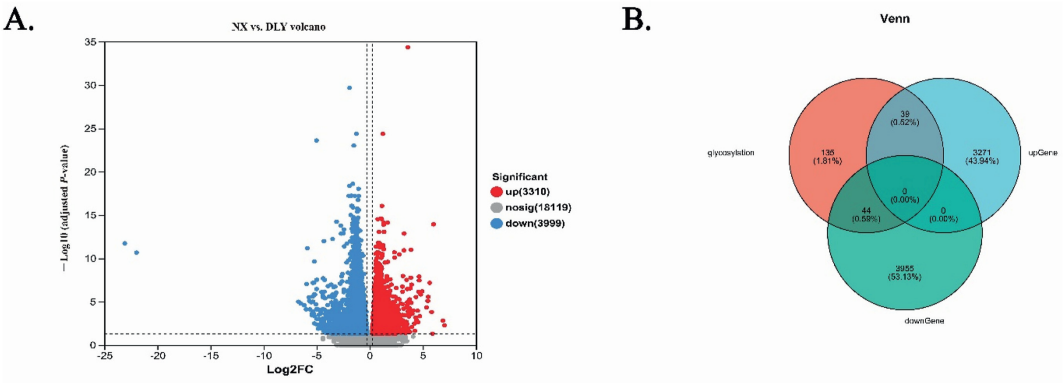

Fig. 3. Transcriptome profile of piglet mucosa. (A) Differential genes; (B) glycosylation-related genes. DLY = Duroc × Landrace × Yorkshire breed; NX = Ningxiang breed; FC = fold change. ** indicates $P < 0.01$, * indicates $P < 0.05$.

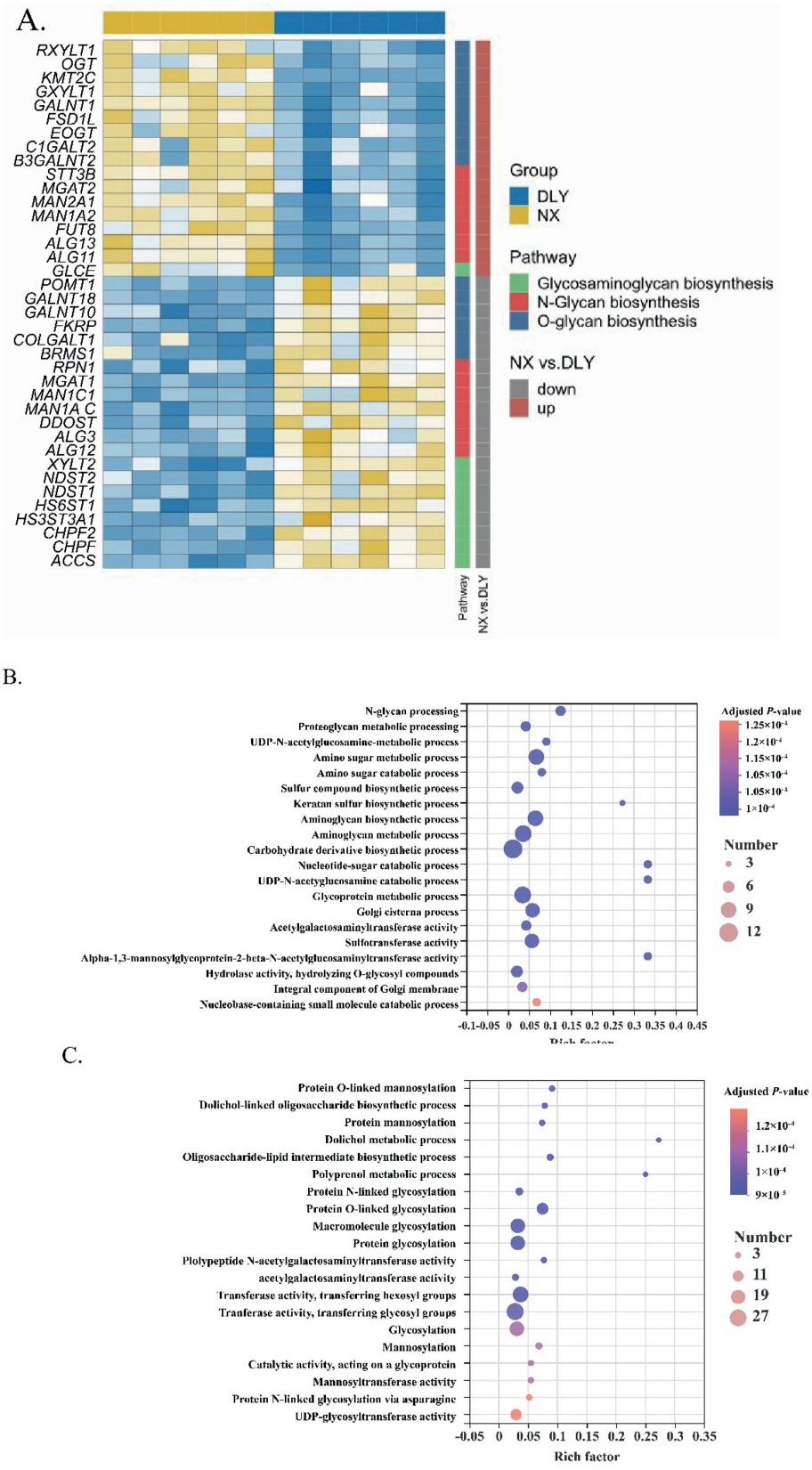

Fig. 4. Differential expression and functional analysis of glycosylation-related genes in the colonic mucosa of DLY and NX Piglets. Distribution characteristics of glycosylation DEGs in the colonic mucosa of the 2 breed piglets (A). Functional analysis of up-regulated glycosylated DEGs in DLY piglets (B) or NX piglets (C), respectively. Differential gene expression of glycosylation (D). DLY = Duroc × Landrace × Yorkshire breed; NX = Ningxiang breed; UDP = uridine diphosphate. * indicates $P < 0.05$.

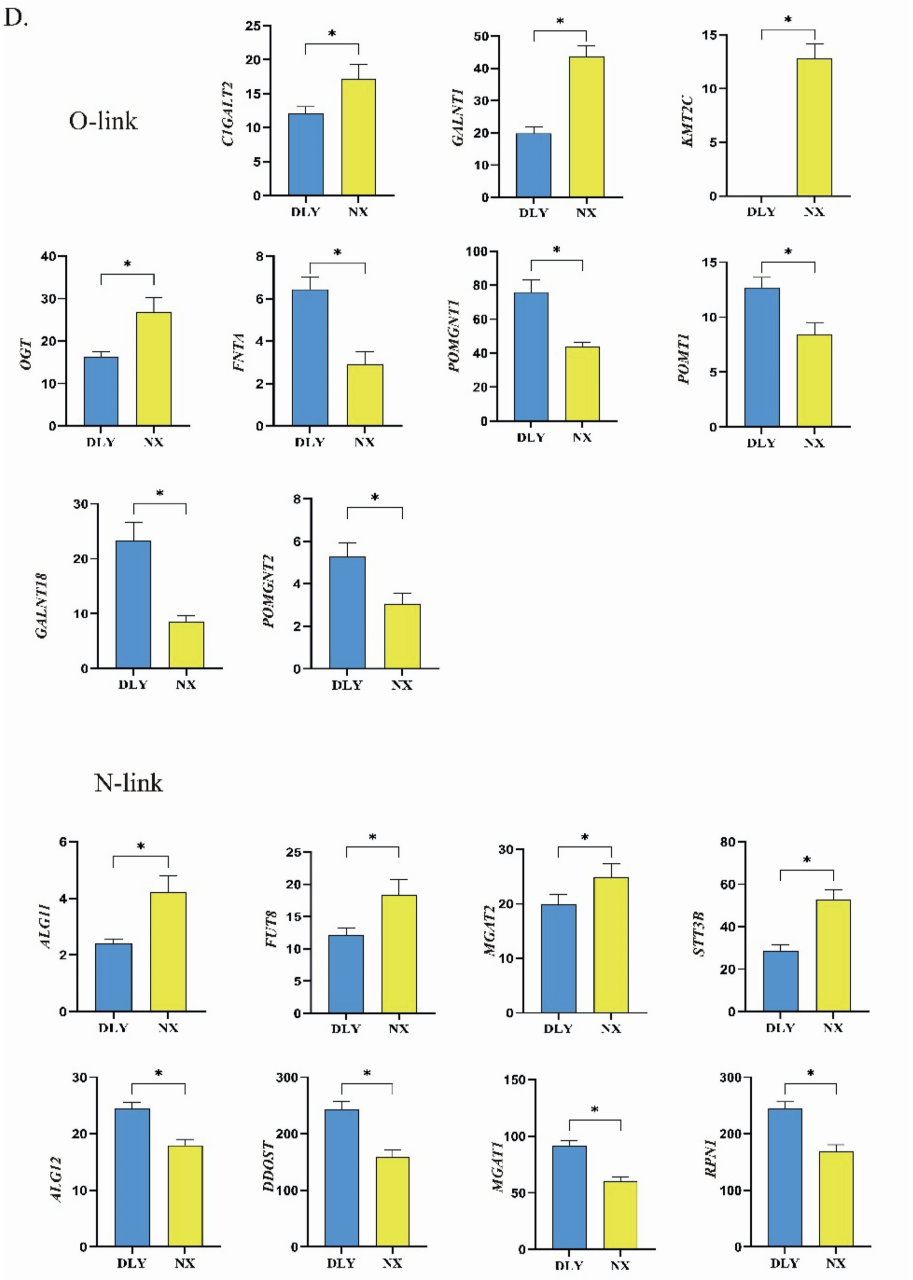

Fig. 4. (*continued*).

piglets and DLY piglets. The results showed that the relative dominant bacteria of NX piglets were mainly from *Lactobacillus* and *Prevotella*; including *Lactobacillus_amylovorus (L.amylovorus)*, *Lactobacillus_reuteris (L.reuteris)*, *Lactobacillus_pontis* (*L.pontis*), *Lactobacillus_crispatus* (*L.crispatus*), *Lactobacillus_helveticus* (*L.helveticuss*), *Prevotella_sp_P5_92 (P.P5_92)*, *Prevotella_sp_P2_180*, *Prevotella_sp_P3_122* and *Prevotella_sp_CAG_604 (P.CAG_604)* (Fig. 6C). NX piglets also had a higher relative abundance of *Subdoligranulum_sp* and *Eubacterium_sp_CAG_180* (*E.CAG_180*) in species-level than DLY piglets. The relative dominant bacteria of DLY piglets included members of *Collinsella, Clostridiales, Streptococcus* and *Enterobacteriaceae*, such as *E.coli, Collinsella_sp, Streptococcus_gallolyicus and Collinsella_aerofaciens* (*C.aerofaciens*) (Fig. 6C).

3.7. Potential "microbe-glycosylation" axis in piglet colonic mucosa

We explored the correlation between gut differential bacteria and O-linked glycosylation DEGs, as depicted in Fig. 7A. Notable correlations were observed between specific bacteria and glycosylation genes. For instance, *C1GALT2* exhibited a significant positive correlation with *L.crispatus*, *P.CAG_604* and *unclassified_Lactobacillus*. GALNT1 was significantly negatively correlated with *E.coli, C.aerofaciens*, *unclassified_Collinsella* and significantly positively correlated with *L.pontis and P.CAG_604*. KMT2C was significantly negatively correlated with *E.coli, C.aerofaciens, unclassified_Enterobacteriaceae* and significantly positively correlated with *L.pontis*, *E.CAG_180*, and *P.CAG_604*. *OGT* was significantly positively correlated with *L.amylovorus*,

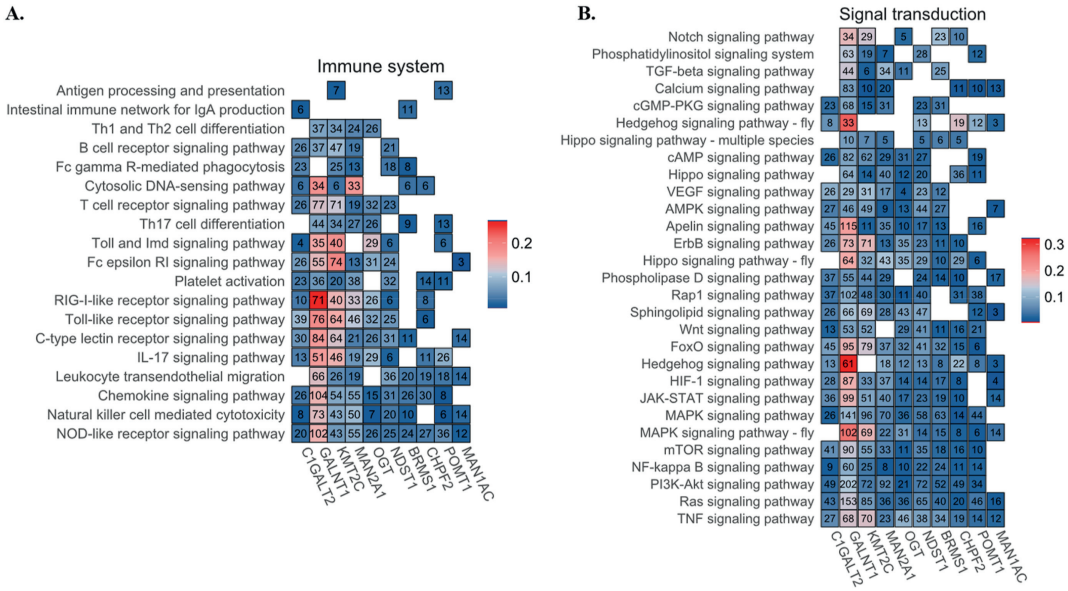

Fig. 5. Signaling pathway of differential glycosylation genes. (A) Immune system; (B) signal transduction NOD. The values in the boxes represent the number of genes associated with the target gene in the pathway. The value on the right represents the proportion of significantly associated genes relative to the total number of associated genes. DLY = Duroc × Landrace × Yorkshire breed; NX = Ningxiang breed; IgA = immunoglobulin A; cGMP-PKG = cyclic guanosine monophosphate-protein kinase G; VEGF = vascular endothelial growth factor; AMPK = adenosine 5′-monophosphate -activated protein kinase.

*L.amylovorus*_CAG.719, *L.crispatus*, *L.helveticuss*, *P.CAG_604* and *unclassified Lactobacillus*.

To illustrate the complex interactions between gut bacteria, *GALNT1*|*KMT2C*, and their co-associated signaling genes, we employed a Sankey plot (Fig. 7B). A total of 73 genes were associated with the gut microbiota, and *KMT2C* and *GALNT1* were commonly linked to 69 of these genes. Most of the genes were associated with ≥2 intestinal differential bacteria. In particular, *L.pontis* had 20 unique related genes. Furthermore, we conducted functional analysis for the co-associated genes of *GALNT* and the microbiota based on the KEGG database (Fig. 7C). Several signaling pathways exhibited close associations with *GALNT*, including the MAPK signaling pathway in flies, TNF signaling pathway, MAPK signaling pathway, FoxO signaling pathway, and JAK-STAT signaling pathway. These pathways involved 125, 90, 70, 69, and 50 mRNAs, respectively, with rich factor values reaching 0.28, 0.23, 0.1, 0.16, and 0.15, respectively.

4. Discussion

After carefully controlling for differences in diet and environment, our study revealed substantial differences in the growth performance and diarrhea rates between Western-style DLY piglets and native Chinese NX pigs at 1 week after weaning. These baseline data suggested that NX piglets had much milder symptoms of post-weaning stress than DLY piglets, with unimpeded growth and lower diarrhea rates. Similar results appeared in the study by (Ma et al., 2022), which reported the low diarrhea rate characteristics of piglets native to China, including Tibet, BeiJingHei, BaMa, and NX, relative to DLY piglets. Davison (2017) also reported that local pigs are better adapted than the exotic breeds and may thus better withstand some of the negative impacts of climate change. After a long period of natural selection, local pigs may have a strong ability to adapt to the environment.

The results of PAS staining, reflecting the total carbohydrate synthesis or secretion of the tissue, showed that NX piglets had more intense PAS staining in their colonic mucosa compared to DLY piglets (Zhai et al., 2022). This suggests that the intestinal mucosa of NX piglets was more actively synthesizing or secreting carbohydrates. Mucins, secreted glycoproteins primarily produced by goblet cells, represent vital components of intestinal mucosa. MUC2, MUC5AC and MUC5B belong to secretory mucins, which are the main components of mucus and participate in various biological functions such as cell adhesion, physical barriers and immune response. In our study, we examined the expression of 3 types of secreted mucins: MUC2, MUC5AC, and MUC5B. The transcriptomic data revealed consistent expression patterns with previous research, with an average expression of (94 ± 2)% for MUC2, (4 ± 0.5)% for MUC5AC, and (2 ± 0.3)% for MUC5B (Xia et al., 2022). However, the transcript expression of MUC5AC and total secreted mucin was higher in DLY piglets than in NX piglets, which seemed to be contrary to the microscopic morphology observations. The synthesis and secretion of mucin is the stress response of the intestinal mucosa to the stimulation, and the upregulation of the mucin gene in DLY piglets is consistent with this logic (Xia et al., 2022). Therefore, there has been a possibility that terrible deterioration arose in the mucosal glycosylation profile of DLY piglets.

Undoubtedly, our study uncovered significant differences in the glycosylation profiles of the transcriptomes between NX piglets and DLY piglets. Notably, *C1GALT2*, which exhibited reduced expression in DLY piglets, is an iso-chaperone gene of the mucin core one synthase gene *C1GALT1*. This reduction in *C1GALT2* expression might reflect a decreased synthesis of core one type mucin in DLY piglets. Strikingly, Similar results were seen in human IBD patients, with patients showing decreased expression of C1GALT2 and colonic core 1 type mucin (Mcgovern et al., 2015; Momozawa et al., 2018). These findings may provide insights into the mechanisms underlying mucosal barrier dysfunction in both pigs and humans, highlighting the importance of *C1GALT2* in maintaining intestinal health. Additionally, our study identified down-regulated fucosylation genes in DLY piglets, mirroring findings in IBD patients. Alternatively, alpha-(1,6)-fucosyltransferase (FUT8), a glycosyltransferase that adds fucose to N-linked sugar chains in colonic mucosa, is elevated in NX piglets. Fucosylation is thought to increase the anti-infection ability of mucins against specific pathogens, so the low

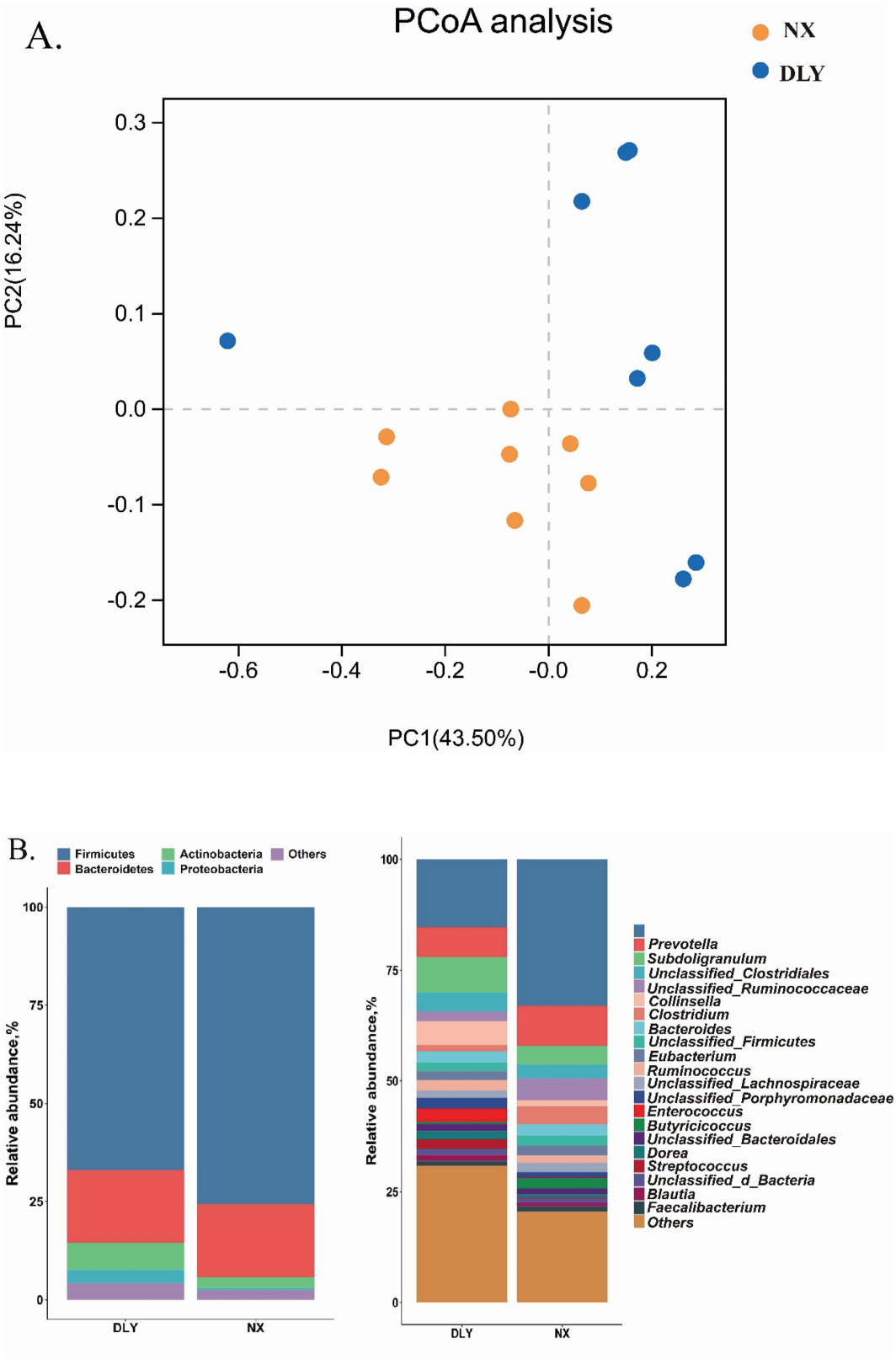

Fig. 6. The microbiome of NX and DLY piglets in colon. (A) Principal coordinate analysis (PCoA); (B) phylum and genus levels; (C) linear discriminant analysis effect size (LEfSe) analysis. DLY = Duroc × Landrace × Yorkshire breed; NX = Ningxiang breed; LDA = linear discriminant analysis.

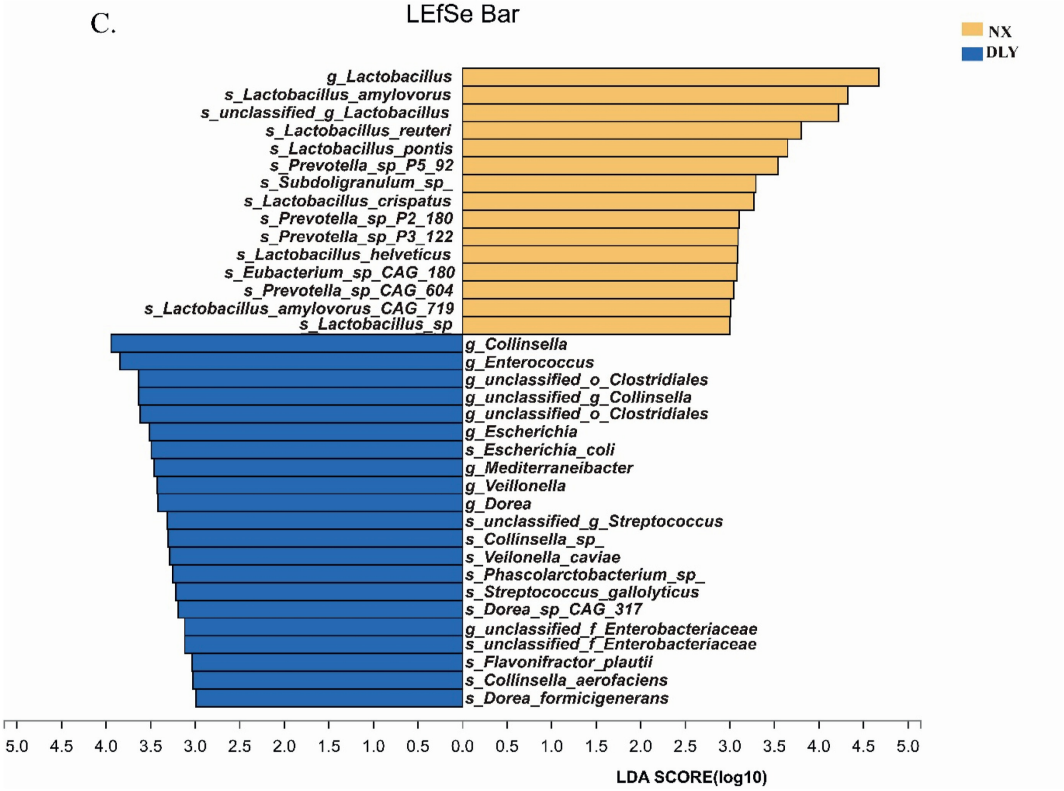

Fig. 6. (*continued*).

expression of FUT8 may lead to a further decline in intestinal barrier function in post-weaned DLY piglets (Qu et al., 2021).

Importantly, our study also highlighted the diminished expression of 2 critical genes, *GALNT1* and *KMT2C*, in DLY piglets. These genes play a pivotal role in catalyzing the O-linking reaction of glycans with mucins. Particularly, the expression of *KMT2C* was almost non-existent in DLY piglets. Loss of *GALNT* gene expression, resulting in a reduction in mucin-linked O-glycans, may be the worst lesions in the glycosylation profile of the intestinal mucosa for DLY piglets (Kato et al., 2021). Since the quantity of O-linked glycans is essential for the functioning of mucins, this reduction might result in a decreased defense capacity of the mucus layer against external stimuli and could significantly impact the composition of the microbiota colonizing the intestinal mucosa (Groux et al., 2020; Nagao et al., 2020). It's worth noting that similar reductions in *GALNT* gene expression and O-linked sugars have been reported in the gut of patients with Ulcerative Colitis (UC) (Hasnain et al., 2017).

Based on the random forest regression model, we identified associated genes of glycosylation DEGs that were significantly enriched in the immune system or signal transduction categories of the KEGG pathway database. Many high-rich factor pathways have been mentioned in previous studies to be related to gut glycosylation profiles, such as the chemokine signaling pathway, Toll-like receptor signaling pathway, IL-17 signaling pathway, JAK-STAT signaling pathway, MAPK signaling pathway and the PI3K-Akt signaling pathway (Qu et al., 2021). Furthermore, the current study also suggested that some new pathways may be closely related to the glycosylation profile of the gut, such as the RIG-I-like receptor signaling pathway, C-type lectin receptor signaling pathway, Cytosolic DNA-sensing pathway, NOD-like receptor signaling pathway, Apelin signaling pathway, ErbB signaling pathway, Hedgehog signaling pathway-fly and the Hedgehog signaling pathway. These findings suggest that glycosylation may play different roles in various cellular processes (Chun et al., 2019). However, it is important to note that many of these new associations require further research and validation.

In particular, inflammation-related cytokines may be potential upstream regulators of *GALNT1* and *KMT2C* expression levels, given the high correlation of the IL-17 signaling pathway, chemokine signaling pathway, and the TNF signaling pathway. Previous studies have reported that gut microbiota regulates the expression of cytokines such as IL-22 through toll-like receptor (TLR) ligands (such as lipopolysaccharides), short chain fatty acids (SCFAs), and tryptophan derivatives, which in turn activate STAT signaling in intestinal mucosal cells to regulate the expression of glycosylation genes (Qu et al., 2021; Bets et al., 2022; Singh et al., 2024). However, further validation studies are needed. Consequently, our pathway prediction results suggest a strong potential correlation between gut microbiota and the gene expression of *GALNT1* and *KMT2C*.

Gut microbes are known to be closely associated with intestinal mucins and play a vital role in shaping the gut environment. Intestinal mucins provide nutrients and a stable habitat for microorganisms, which in turn regulate mucin production through feedback mechanisms to maintain intestinal barrier function (Juge et al., 2024). The current study examined the colonic microbiome of DLY and NX piglets using metagenomic sequencing, from which significant differences were captured based on PCoA. NX piglets had more dominant *Lactobacillus* members than DLY piglets, including *L.amylovorus*, *L.reuteris*, *L.pontis*, and *Prevotella* members, including *P.P5_92*, *P.P2_108*, and *P.CAG_604*. *Lactobacillus* is the most common dominant bacteria in the gut of weaned piglets, maintaining the homeostasis of gut microecology in such young piglets (Gresse et al., 2017). *Prevotella* was the most important contributor of polysaccharide lyases in the piglet gut microbiota in the current

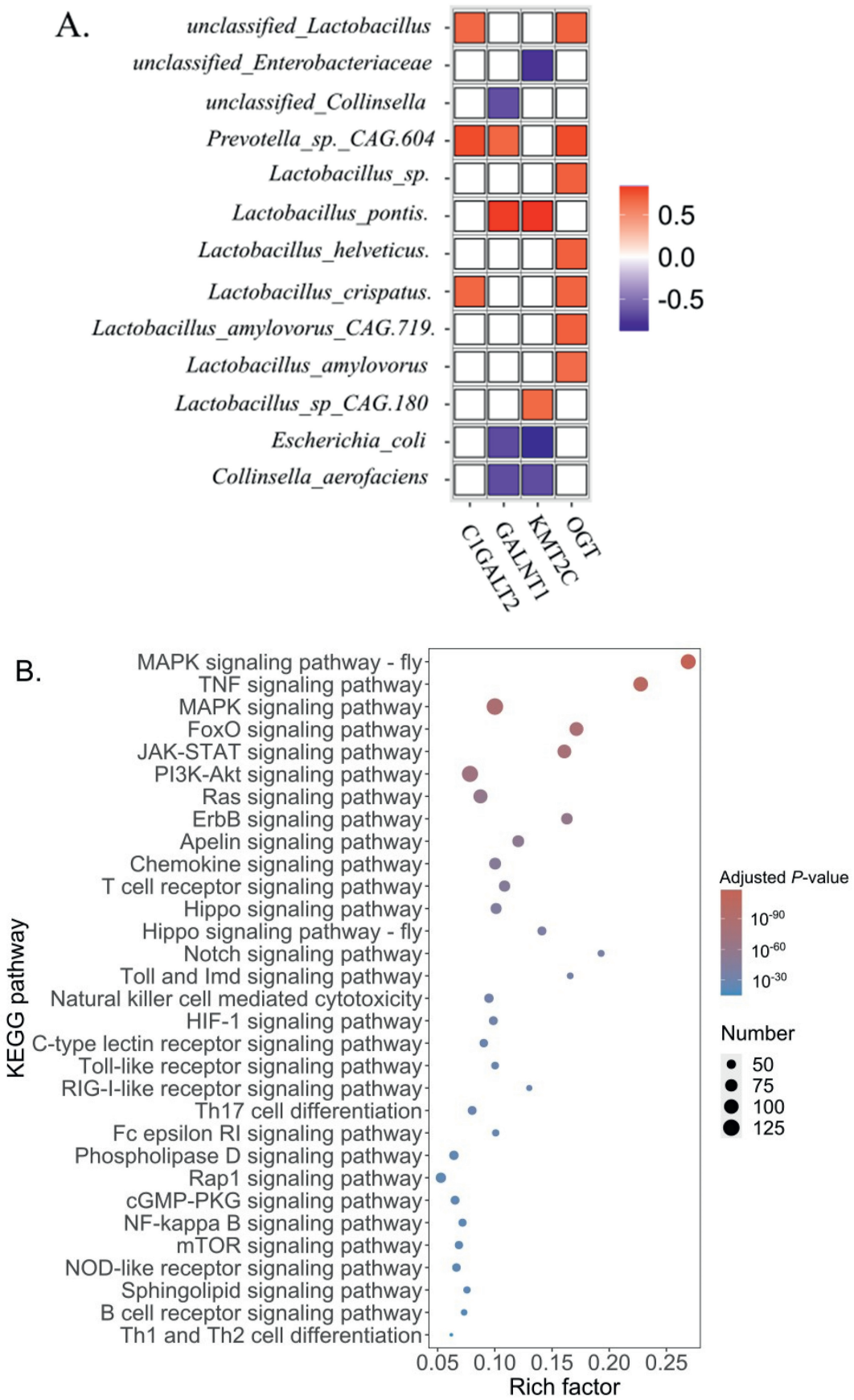

Fig. 7. The relationship between the microbiome and glycosylated mucin. (A) Association between differential microbiota and differential glycosylation genes, the color red indicates a positive correlation between the bacteria and genes, while blue represents a negative correlation; (B) Signal enrichment of *GALNT1*; (C) Association of *KMT2C* and *GALNT1* with differential bacterial strains. DLY = Duroc × Landrace × Yorkshire breed; NX = Ningxiang breed.

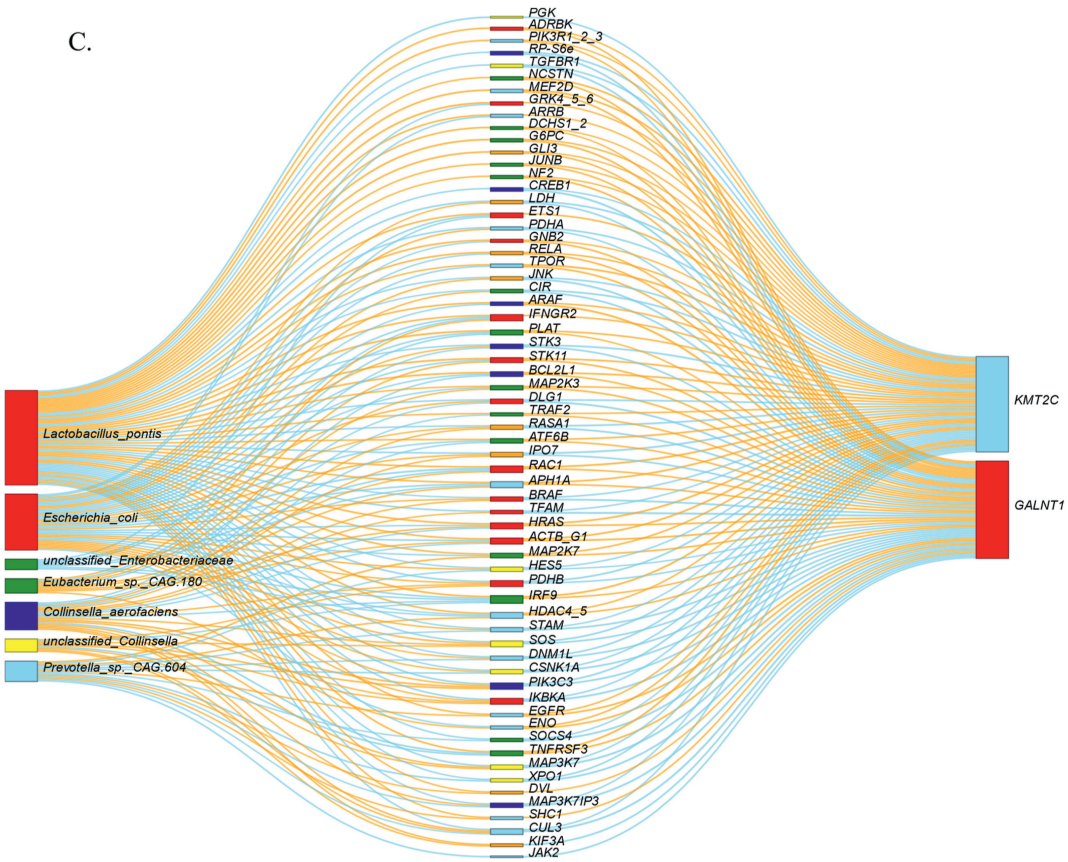

Fig. 7. (*continued*).

study (Zhou et al., 2020). The dominant *Prevotella* member may be related to the response of the microbiota to plant-derived feed (Chen et al., 2017). Similar results for the gut microbiota of NX piglets were presented in our previous study (Li et al., 2021). Conversely, DLY piglets exhibited a dominance of opportunistic pathogens, with genera like *Escherichia* and *Collinsella*, including *E.coli* and *C.aerofaciens*, being particularly prevalent. These opportunistic pathogens have the potential to induce stress in the intestinal mucosa by releasing TLR ligands, triggering an immune response (Gresse et al., 2017). These observations underscore the critical role of gut microbiota in influencing the intestinal environment and, consequently, the glycosylation profiles observed in piglets.

Spearman correlation analysis provided further insights into the relationship between microbiota and the expression of *GALNT1* and *KMT2C* genes. Notably, it revealed that dysbiosis in the microbiota was associated with the downregulation of *GALNT1* and *KMT2C*. Among the 4 O-linked glycosylation genes closely related to microbiota, only *GALNT1* and *KMT2C* negatively correlated with harmful bacteria such as *E. coli* and *C.aerofaciens*. This suggests that the reduced O-linked glycans observed in the intestinal mucosa of DLY piglets may be linked to the proliferation of these detrimental bacteria, a finding consistent with observations in patients with IBD (Hasnain et al., 2017). Fortunately, beneficial bacteria are positively associated with *GALNT1* or *KMT2C*, *L.pontis*, *P.CAG_604*, and *E.CAG_180*. These beneficial bacteria may promote the expression of *GALNT1* or *KMT2C* through different pathways, such as the production of SCFAs to inhibit the pro-inflammatory response of the above-mentioned harmful bacteria (Gresse et al., 2017). This underscores the importance of maintaining a balanced microbiota for intestinal health and provides a potential target for therapeutic interventions in conditions such as IBD.

To gain a more comprehensive understanding of this intricate relationship between microbiota and glycosylation genes, we identified potential intermediate genes using a Sankey plot. Most intermediate genes were associated with $\geq$2 bacteria, further suggesting the importance of the relative balance of beneficial and harmful bacteria in the microbiota for the GALNT gene. Our analysis highlighted the crucial roles of pathways such as the MAPK signaling pathway, TNF signaling pathway, FoxO signaling pathway, and JAK-STAT signaling pathway in mediating the interaction between the microbiota and *GALNT* genes, as indicated by functional analysis based on the KEGG database. A visual representation of these findings is presented in Fig. 7B.

Of particular interest, *L.pontis*, *Lactobacillaceae* identified only in the NX piglet gut, has multiple intermediate genes that are independently linked. It could be speculated that *L.pontis* may have the ability to improve the glycosylation profile of piglets based on the above results. Unfortunately, these intermediate genes did not yield significant results in functional analysis. Future research should focus on validating the potential of *L.pontis* derived from Ningxiang pigs to improve the glycosylation profile of weaned piglets and elucidate the underlying mechanisms.

5. Conclusions

The study identified the transcriptional profile and glycosylation signature of weaned piglets from 2 different breeds. By comparing differentially glycosylated genes and their functions, we have identified that the low expression of GALNT1 and KMT2C genes,

responsible for catalyzing O-linked reactions of proteins and glycans, could severely compromise the intestinal barrier function in DLY piglets. Additionally, *Lactobacillus* and *Prevotella* members appear to play an active role in shaping the glycosylation profile of piglet colons, while *E. coli* and *C.aerofaciens* members have the opposite effect. Furthermore, the dominant *L.pontis* strain specific to NX piglets holds promise as a potential probiotic capable of modulating the glycosylation profile of piglet intestinal mucosa. Further investigations are warranted to confirm these findings and explore the mechanisms involved.

CRediT authorship contribution statement

Hao Cheng: Writing – original draft. **Hao Li:** Writing – original draft. **Yujie Zhao:** Investigation. **Kai Yang:** Investigation. **Jing Wang:** Supervision. **Bie Tan:** Funding acquisition. **Xiaokang Ma:** Funding acquisition.

Declaration of competing interest

We declare that we have no financial and personal relationships with other people or organizations that can inappropriately influence our work, and there is no professional or other personal interest of any nature or kind in any product, service and/or company that could be construed as influencing the content of this paper.

Acknowledgements

This research was supported by the National Natural Science Foundation of China (32202692 and U22A20510), the Hunan Provincial Natural Science Foundation of China (2022JJ40176).

Appendix Supplementary data

Supplementary data to this article can be found online at https://doi.org/10.1016/j.aninu.2024.12.001.

References

Arora K, Sherilraj PM, Abutwaibe KA, Dhruw B, Mudavath SL. Exploring glycans as vital biological macromolecules: a comprehensive review of advancements in biomedical frontiers. Int J Biol Macromol 2024;268(1):131511.

Bets VD, Achasova KM, Borisova MA, Kozhevnikova EN, Livinova EA. Role of mucin-2 glycoprotein and L-fucose in interaction of immunity and microbiome within the experimental model of inflammatory bowel disease. Biochemistry 2022;17(4):301–18.

Chen T, Long W, Zhang C, Liu S, Zhao LP, Hamaker BR. Fiber-utilizing capacity varies in Prevotella-versus Bacteroides-dominated gut microbiota. Sci Rep 2017;7(1):2594.

China Feed Database. Tables of feed composition and nutritive values in China. https://www.chinafeeddata.org.cn/admin/Login/slcfb. [Accessed 10 October 2019].

Chun SH, Oh NS, Lee JY, Lee KW. Anti-inflammatory activities of Maillard reaction products from whey protein isolate fermented by Lactobacillus gasseri 4M13 in lipopolysaccharide-stimulated RAW264. 7 cells. J Dairy Sci 2019;102(9):7707–16.

Cummings RD. Stuck on sugars–how carbohydrates regulate cell adhesion, recognition, and signaling. Glycoconj J 2019;36:241–57.

Cummings RD, Pierce JM. The challenge and promise of glycomics. Chem Biol 2014;21(1):1–15.

Davison M. Comparison of febrile responses, thermoregulation and skin morphology in the local kolbroek, windsnyer and exotic large white breeds of pigs in South Africa. University of the Witwatersrand, Faculty of Health Sciences; 2017.

Demirturk M, Cinar MS, Acvi FY. The immune interactions of gut glycans and microbiota in health and disease. Mol Microbiol 2024;00:1–18.

Earley H, Lennon G, Balfe A, Coffey JC, Winter DC, O'Connell PR. The abundance of Akkermansia muciniphila and its relationship with sulphated colonic mucins in health and ulcerative colitis. Sci Rep 2019;9:15683.

Frese SA, Parker K, Calvert CC, David AM. Diet shapes the gut microbiome of pigs during nursing and weaning. Microbiome 2015;3(1):1–10.

Gresse R, Chaucheyras-Durand F, Fleury MA, Wiele TVF, Blanquet S. Gut microbiota dysbiosis in postweaning piglets: understanding the keys to health. Trends Microbiol 2017;25(10):851–73.

Gresse R, Chaucheyras-Durand F, Duniere L, Blanquet S, Forano E. Microbiota composition and functional profiling throughout the gastrointestinal tract of commercial weaning piglets. Microorganisms 2019;7(9):343.

Groux-Degroote S, Cavdarli S, Uchimura K, Allain K, Delannoy P. Glycosylation changes in inflammatory diseases. Adv Prot Chem Struct Biol 2020;119:111–56.

Goto Y, Obata T, Kunisawa J, Sato S, Ivanov I, Lamichhane A, Takeyama N, Kamioka M, Matsuki T, Setoyama H, Imaoka A, Uematsu S, Akira S, Domino S, Kulig P, Becher B, Renauld J, Sasakawa C, Umeasaki Y, Benno Y, Kiyono H. Innate lymphoid cells regulate intestinal epithelial cell glycosylation. Science 2014;345(6202):1254009.

Han XB, Hu XD, Jin W, Liu G. Dietary nutrition, intestinal microbiota dysbiosis and post-weaning diarrhea in piglets. Anim Nutr 2024;17:188–207.

Hasnain SZ, Dawson PA, Lourie R, Hulson P, Tong H, Grencis RK, McGuckin MA, Thornton DJ. Immune-driven alterations in mucin sulphation is an important mediator of Trichuris muris helminth expulsion. PLoS Pathog 2017;13(2):e1006218.

Juge N, Latousakis D, Crost EH. Host mucin glycosylation and gut symbiosis. Transl Glycobiol Hum Health Dis 2024:153–73.

Kato K, Hansen L, Clausen H. Polypeptide n-acetylgalactosaminyl transferase-Associated phenotypes in mammals. Molecules 2021;26(18):5504–22.

Kawashima H. Roles of the gel-forming Muc2 mucin and its o-glycosylation in the protection against colitis and colorectal cancer. Front Tumor Glycobiol 2012;35:1637–41.

Kostic AD, Xavier RJ, Gevers D. The microbiome in inflammatory bowel disease: current status and the future ahead. Gastroenterology 2014;146(6):1489–99.

Kudelka MR, Stowell SR, Cummings RD, Neish AS. Intestinal epithelial glycosylation in homeostasis and gut microbiota interactions in IBD. Nat Rev Gastroenterol Hepatol 2020;17(10):597–617.

Li Y, Sun T, Hong Y, Qiao T, Wang YS, Li W, Tang S, Yang X, Li J, Li XW, Zhou ZT, Xiao YC. Mixture of five fermented herbs (Zhihuasi Tk) alters the intestinal microbiota and promotes the growth performance in piglets. Front Microbiol 2021;12:725196.

Ma N, Sun Y, Chen J, Qi ZK, Liu CC, Ma X. Micro-coevolution of genetics rather than diet with enterotype in pigs. Front Nutr 2022;9:846974.

McGovern DPB, Kugathasan S, Cho JH. Genetics of inflammatory bowel diseases. Gastroenterology 2015;149(5):1163–76.

Momozawa Y, Dmitrieva J, Theatre E, Deffontaine V, Rahmouni S, Charloteaux B, Crins F, Docampo E, Elansary M, Gori AS, Lecut C, Mariman R, Mni M, Oury C, Altukhov I, Alexeev D, Aulchenko Y, Amininejad L, Bouma G, Hoentjen F, Lowenberg M, Oldenburg B, Pierik MJ, Meulen-deJong AE, Woude CJ, Visschedijk MC, Lathrop M, Hugot JP, Weersma RK, Vos MD, Franchimont D, Vermeire S, Kubo M, Louis E, Georges M. IBD risk loci are enriched in multigenic regulatory modules encompassing putative causative genes. Nat Commun 2018;9(1):2427.

Morgan XC, Tickle TL, Sokol H, Gevers D, Devaney KL, Ward DV, Reyes JA, Shah SA, Leleiko N, Snapper SB, Bousvaros A, Korzenik J, Sands BE, Xavier RJ, Huttenhower C. Dysfunction of the intestinal microbiome in inflammatory bowel disease and treatment. Genome Biol 2012;13(9):1–18.

Neelamegham S, Mahal LK. Multi-level regulation of cellular glycosylation: from genes to transcript to enzyme to structure. Curr Opin Struct Biol 2016;40:145–52.

Nagao-Kitamoto H, Leslie JL, Kitamoto S, Jin CS, Thomsson KA, Merritt G, Gillilland I, Kuffa P, Goto Y, Jenq RR, Ishii C, Hirayama A, Seeekatz AM, Martens EC, Eaton KA, Kao JY, Fukuda SJ, Higgins PDR, Karlsson NG, Young VB, Kamada N. Interleukin-22-mediated host glycosylation prevents Clostridioides difficile infection by modulating the metabolic activity of the gut microbiota. Nat Med 2020;26(4):608–17.

NRC. Nutrient requirements of swine. 11th revised ed. Washington (DC): National Academic Press; 2012.

Qu DW, Wang G, Yu LL, Tian FW, Chen W, Zhai QX. The effects of diet and gut microbiota on regulation of intestinal mucin glycosylation. Carbohydrate Polymers 2021;258:117651.

Singh A, Beaupre M, Villegas-Novoa C, Hearing P, Allibritton NL, Kumar P. IL-22 promotes mucin-type O-glycosylation and MATH1^{+} cell-mediated amelioration of intestinal inflammation. Cell Rep 2024;43(5):1–21.

Xia B, Zhong R, Meng Q, Wu WD, Chen L, Zhao X, Zhang HF. Multi-omics unravel the compromised mucosal barrier function linked to aberrant mucin O-glycans in a pig model. Int J Biol Macromol 2022;207:952–64.

Zhai Y, Zheng X, Mao Y, Li K, Liu YH, Gao YM, Zhao MS, Yang R, Chen W. Recombinant Human Thymosin β4 (rhTβ4) Modulates the anti-inflammatory responses to alleviate benzalkonium chloride (BAC)-induced dry eye disease. Int J Mol Sci 2022;23(10):5458.

Zhai YL, Zhou X, Zhang ZQ, Zhang L, Wang DY, Wang XH, Sun W. Design, synthesis, and characterization of schiff base bond-linked pH-responsive doxorubicin prodrug based on functionalized mPEG-PCL for targeted cancer therapy. Polemers 2018;10(10):1127.

Zhou SS, Luo RB, Gong G, Wang YF, Ge SZM, Wang K, Xu ZF, Suo LSZ. Characterization of metagenome-assembled genomes and carbohydrate-degrading genes in the gut mictobiota of Tibetan pig. Front Mictobiol 2020;11:1–11.